Oxidation States of Ytterbium Incorporated in Calcium Carbonate and Calcium Fluoride

Tetsuaki Yoshida, Hiroyuki Kagi,* Hiroshi Tsuno,† Atsuyuki Ohta,†† and Masaharu Nomura†††
Laboratory for Earthquake Chemistry, Graduate School of Science, The University of Tokyo, Tokyo 113-0033
†*Institute for Environmental Management Technology, AIST, Ibaraki 305-8569*
††*Geological Survey of Japan, AIST, Ibaraki 305-8567*
†††*Institute of Materials Structure Science, KEK, Ibaraki 305-0801*

(Received March 3, 2005; CL-050282)

Divalent ytterbium was found in great amounts in calcium carbonate polymorphs (calcite and aragonite) and calcium fluoride, and the Yb^{2+}/Yb^{3+} ratios in these materials increased with increasing saturation states of the respective starting solutions.

Valence of lanthanide elements is dominated by the +3 oxidation state in aqueous solution at room temperature except for Ce^{4+} and Eu^{2+}.[1,2] Recently, we reported the occurrence of Yb^{2+} in synthetic Yb-doped calcite ($CaCO_3$);[3] nevertheless, Yb^{2+} is not thermodynamically stable in aqueous solutions. Similarly, Sidike et al. reported photoluminescence (PL) and excitation spectra of natural fluorite (CaF_2) from Okayama prefecture, Japan: that fluorite also showed the presence of Yb^{2+}.[4] The present study uses X-ray absorption near-edge structure (XANES) technique to investigate the oxidation state of Yb incorporated in calcium-carbonate polymorphs and calcium fluoride. Thereby, we elucidate the formation mechanism of Yb^{2+} in these materials.

We prepared Yb-doped calcium-carbonate polymorphs, calcite, aragonite as follows. Calcite was precipitated from a 1:1 mixture of $CaCl_2$ and $NaHCO_3$ solutions (each 30 mM (mol kg^{-1})) containing 5 μM $YbCl_3$. The mixed solution in a glass vessel was closed with a silicon plug and stirred with a magnetic stirrer at 30 °C for one day. Aragonite was precipitated from a mixed solution of $CaCl_2$, $NaHCO_3$ (each 30 mM), $MgCl_2$ (25 mM), and 0.5 μM $YbCl_3$. The precipitates were filtered with a membrane filter (25 mm diameter and 0.45 μm pore size, Millipore® HAWP02500; Millipore Corp.) then rinsed with milli-Q® water. The precipitates were dried at 100 °C in air for 30–60 min. Yb-doped calcium fluoride was precipitated from a mixed solution of 0.1 M (mol kg^{-1}) of $Ca(NO_3)_2$, 0.2 M of NaF, and 5 μM of $YbCl_3$ in a glass vessel.[5] After standing for one day, the supernatant was removed. Then the precipitate was dried at 100 °C in air for 3–5 h.

The obtained samples were identified using a powder X-ray diffractometer (MiniFlex; Rigaku Corp.). Concentrations of Yb incorporated in the samples were determined by using an ICP atomic emission spectrometer (SPS 1200A; Seiko Instruments Inc.) after decomposition with 0.1 M HNO_3. The respective Yb/Ca molar ratios in calcite, aragonite and CaF_2 were approximately 1.2×10^{-3}, 1.8×10^{-4}, and 8.8×10^{-5}.

XANES spectra were collected in fluorescence mode at the beamline BL12C of the Photon Factory, High Energy Accelerator Research Organization (KEK-PF) in Tsukuba, Japan.[6] Measurements in the fluorescence mode enable the detections of trace Yb in the samples. A Si(111) double-crystal monochromator was used. Its beam, smaller than 1 mm^2, was focused using a bent cylindrical mirror. The Yb L_{III} (8947 eV) absorption of samples was recorded by the fluorescence yield (Yb Lα: 7.4 keV) using a 19-element pure Ge solid-state detector. Single-channel analyzers (SCA) selected the energy region around Yb fluorescence. The monochromator was calibrated at 8947 eV (Yb L_{III} absorption edge) using ytterbium oxide powder. The incident X-ray intensity (I_0) was monitored using an ion chamber filled with nitrogen gas. The X-ray absorption (μ) is expressed as $\mu = I_f/I_0$ (I_f is the fluorescence X-ray intensity and μ is plotted against the incident X-ray energy. For each sample, 3–5 scans were conducted.

The XANES spectra were analyzed using a computer program (REX2000; Rigaku Corp.). The main peak (around 8947 eV) and shoulder peak (around 8940 eV) of Yb L_{III}-edge XANES spectra (see Figures 1a and 1b) can be fit by a combination of a Lorentzian function for the white line and an arctangent function for the continuum absorption, respectively.[7] Four parameters: peak position, peak height, full width at half maximum (FWHM) of the Lorentzian curve, and arctangent curve height were optimized for each paek by the least square method at an energy range of 8920–8960 eV. In the fitting procedure, the height ratio of Lorentzian curve to the arctangent curve was kept constant for Yb^{2+} and Yb^{3+} peaks.

Figures 1a and 1b show the Yb L_{III}-XANES spectra for Yb-doped calcite and aragonite and the results of peak fitting. These spectra had a main white line (around 8947 eV) which is assigned to the electron transition $2p \rightarrow 5d6s$ of Yb^{3+}.[8,9] Additionally, shoulder was discerned in the low-energy side of the main peak (around 8940 eV). The shoulder peak position was consistent with that of Yb^{2+} reported for Yb-bearing compounds.[8,9] Tanaka et al. estimated the molar ratio of Yb^{2+} and Yb^{3+} directly from the intensity ratio of the two peak areas.[7] For the materials examined herein, the large amount of Yb^{2+} was incorporated in Yb-doped aragonite prepared in the atmo-

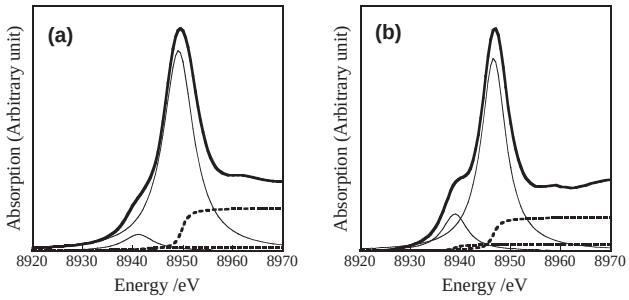

Figure 1. Yb L_{III}-edge XANES and deconvoluted spectra of (a) Yb-doped calcite and (b) Yb-doped aragonite. The bold line represents observed XANES, the thin line represents the Lorentzian function, and the dotted line represents arctangent function.

spheric oxygen pressure. The Yb^{2+}/Yb^{3+} ratio in Yb-doped aragonite was about 0.20 and much higher than that of calcite (about 0.14).

Figure 2a shows XANES spectra of Yb-doped aragonite samples precipitated under three saturation states. The Yb^{2+}/Yb^{3+} ratios of the aragonite samples that were precipitated under the saturation states of $\Omega = 22$ (equivalent to Figure 1b), 18 and 10 were about 0.20, 0.05, and 0.02, respectively. The respective Yb^{2+}/Yb^{3+} ratios in the calcium carbonate increased markedly as the starting solutions' saturation states increased. Similar behavior was observed for CaF_2, as displayed in Figure 2b. The Yb^{2+}/Yb^{3+} ratios incorporated into CaF_2 samples prepared at the saturation states of $\Omega = 2.0 \times 10^7$, $\Omega = 3.0 \times 10^6$, and $\Omega = 5.2 \times 10^5$ were about 0.56, 0.16, and 0.09, respectively. With increasing saturation states, the growth rate and density of lattice defects increase in the grown crystals. Thus, we infer that the increase of the saturation state can increase the respective occurrence of O^{2-} and F^- vacancies in $CaCO_3$ and CaF_2. Occurrence of O^{2-} and F^- vacancies stabilized the Yb^{2+} in Yb-doped $CaCO_3$ and CaF_2 ($2Yb^{3+} + O^{2-} \rightarrow 2Yb^{2+} + V_O{}^{2-} + O$ and $Yb^{3+} + F^- \rightarrow Yb^{2+} + V_{F-} + F$, where V_x represents the vacancy of atom X.).

Figure 3a shows XANES spectra of Yb-doped aragonite samples heated in air for 1 h at temperature of 300, 400, and 500 °C, respectively, followed by quenching to room temperature. The Yb^{2+}/Yb^{3+} ratios in aragonite decreased from 0.20 to 0.09 and 0.05 by heating in air for 1 h at 300 °C and 400 °C, respectively. Finally, no Yb^{2+} was found in XANES spectra of the aragonite sample heated for 1 h at 500 °C. Figure 3b shows XANES spectra of as-grown Yb-doped CaF_2 and of Yb-doped CaF_2 heated in air or H_2 gas. The Yb^{2+}/Yb^{3+} ratios in CaF_2 decreased from 0.56 to 0.33 and 0.28 by heating in air at 500 °C for 1 h and 3 h, respectively (see Figure 3b: (1)–(3)). The oxidation rate of Yb^{2+} in CaF_2 was smaller than that of the aragonite sample. On the other hand, Figure 3b-(4) indicate that the H_2 gas reacted with Yb^{3+} as a strong reducer by heating at 300 °C, thereby markedly increasing the Yb^{2+}/Yb^{3+} ratio (about 0.89). On the other hand, heating in H_2 gas for 1 h at 500 °C decreased the Yb^{2+}/Yb^{3+} ratio (about 0.45, data not shown). Heating in air or in H_2 gas at high temperature induced the recombination of vacancies and interstitial O and F atoms followed by formation of Yb^{3+} from Yb^{2+}. Moreover, heating in air directly oxidized Yb^{2+} to Yb^{3+}, whereas the heating experiments in H_2 reduced Yb^{3+} to Yb^{2+}. Consequently, the interaction between the formation–recombination of lattice defects and the direct oxidation–reduction induced by diffusion of reacting gas compounds altered the valence of Yb in $CaCO_3$ and CaF_2. When heating Yb-doped CaF_2 in H_2 gas at temperature $\geq$500 °C, the recombination of lattice vacancies was dominated and the Yb^{2+}/Yb^{3+} ratio decreased even in the reduced environment. These results imply that formation of Yb^{2+} from Yb^{3+} in these crystals was induced by lattice defects such as vacancies.

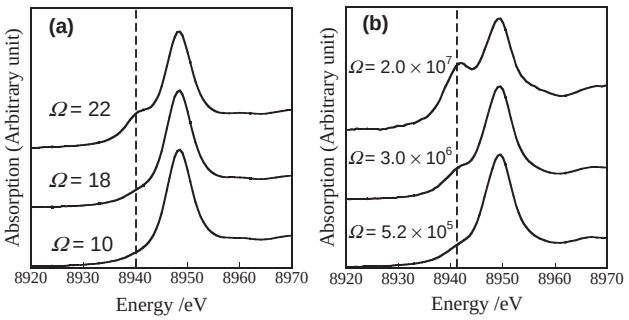

Figure 2. (a) Yb L_{III}-edge XANES of Yb-doped aragonite samples precipitated under saturation states of $\Omega = 22$, 18, and 10. (b) Yb L_{III}-edge XANES of Yb-doped CaF_2 samples precipitated under saturation states of $\Omega = 2.0 \times 10^7$, 3.0×10^6, and 5.2×10^5.

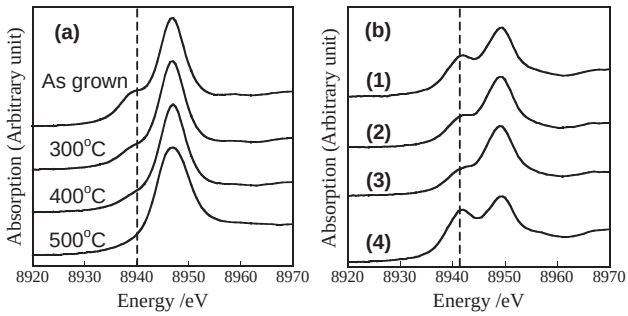

Figure 3. (a) Yb L_{III}-edge XANES of Yb-doped aragonite samples after heating in air for 1 h at temperature of 300, 400, and 500 °C. (b) Yb L_{III}-edge XANES of (1) as-grown Yb-doped CaF_2 samples, (2) after heating in air for 1 h at 500 °C, (3) after heating in air for 3 h at 500 °C, (4) after heating in H_2 gas for 1 h at 300 °C.

In conclusion, Yb incorporated in calcite, aragonite, and CaF_2 synthesized under atmospheric conditions contained a considerable amount of Yb^{2+}. In particular, formation mechanism of Yb^{2+} was considered from aragonite and CaF_2, because Yb^{2+}/Yb^{3+} ratios in these materials were much higher than those in calcite. This study suggested that the reduction of Yb^{3+} was induced by the existence of lattice defects

The XANES experiments were performed under approval of the Photon Factory Program Advisory Committee (2002G257, 2002G275, and 2004G321). This research was supported by Grant-in-Aid (Nos. 14654096 and 15340190) from JSPS.

References

1 S. A. Wood, *Chem. Geol.*, **88**, 99 (1990).
2 M. Bau, *Chem. Geol.*, **93**, 219 (1991).
3 H. Tsuno, H. Kagi, Y. Takahashi, T. Akagi, and M. Nomura, *Chem. Lett.*, **32**, 500 (2003).
4 A. Sidike, I. Kusachi, and N. Yamashita, *Phys. Chem. Miner.*, **30**, 478 (2003).
5 E. Faulques, J. Wery, B. Dulieu, C. Seybert, and D. L. Perry, *J. Fluoresc.*, **8**, 283 (1998).
6 M. Nomura and A. Koyama, *KEK Rep.*, **95-15**, 1 (1995).
7 T. Tanaka, T. Hanada, S. Yoshida, T. Baba, and Y. Ono, *Jpn. J. Appl. Phys.*, **32**, 481 (1993).
8 T. K. Hatwar, R. M. Nayaka, B. D. Padalia, M. N. Ghatikar, E. V. Sampathkumaran, L. C. Gupta, and R. Vijayaraghavan, *Solid State Commun.*, **34**, 617 (1980).
9 C. N. R. Rao, D. D. Sarma, P. R. Sarode, E. V. Sampathkumaran, L. C. Gupta, and R. Vijayaraghavan, *Chem. Phys. Lett.*, **76**, 413 (1980).

Published on the web (Advance View) May 21, 2005; DOI 10.1246/cl.2005.852